H-Bonded and Stacked Dimers of Pyrimidine and *p*-Benzoquinone. A Combined Matrix Isolation Infrared and Theoretical *ab Initio* Study

W. McCarthy,[†] A. M. Plokhotnichenko,[‡] E. D. Radchenko,[‡] J. Smets,[†,§] D. M. A. Smith,[†] S. G. Stepanian,[†,‡] and L. Adamowicz*[,†]

Department of Chemistry, University of Arizona, Tucson, Arizona 85721, Institute for Low Temperature Physics and Engineering National Academy of Sciences of Ukraine, 47 Lenin Avenue, Kharkov 310164, Ukraine, and Department of Chemistry, University of Leuven, Celestijnenlaan 200F, 3001 Heverlee, Belgium

Received: April 29, 1997; In Final Form: July 10, 1997[⊗]

Matrix isolation IR spectroscopy and high-level *ab initio* calculations were applied to investigate the structure and vibrational spectra of quinone−pyrimidine heterodimers formed in low-temperature Ar matrices. A specially developed experimental technique was used to separate bands of quinone−pyrimidine dimer from bands of quinone and pyrimidine monomers and homodimers in the IR spectra. As a result, nine bands assigned to the quinone−pyrimidine heterodimer were identified. *Ab initio* calculations at the MP2/6-31+G*, MP2/6-31++G** and SCF/6-31++G** levels of theory have been carried out to determine the relative energies and vibrational spectra of three stable configurations of the quinone−pyrimidine dimer found theoretically. These configurations are two planar complexes with two weak C−H···O and C−H···N hydrogen bonds and one stacked complex stabilized by dispersion forces. The effect of basis set superposition error (BSSE) on the relative stabilities and the vibrational spectra of the dimers was also investigated. The non-BSSE-corrected calculations at the MP2/6-31+G* and MP2/6-31++G** levels of theory predict the stacked dimer to be the most stable conformer, but accounting for BSSE resulted in a reverse stability ordering of the stacked and the planar dimers. The comparison of the observed frequency shifts with the theoretically predicted shifts has shown that the planar configuration is responsible for the experimentally observed bands. This is in agreement with the stability ordering derived from the BSSE-corrected relative energies. To account for the matrix effects on the stability of the planar and stacked dimers, additional calculations were carried out using the Onsager's reaction field model and the MP2/6-31++G** level of theory. These calculations confirm that the planar H-bonded dimer is the most stable configuration.

1. Introduction

Weak interactions give important contributions to the stabilization of the structure of various forms of DNA and RNA.[1] It is well known that the helical structure of DNA is stabilized not only by H-bonds in Watson−Crick AT and GC pairs, but also by stacking interactions between pyrimidine and purine bases along the DNA helical backbone. Recently, Murphy *et al.*[2] found that stacked heterocycles of DNA serve as an efficient medium for coupling electron donors and acceptors over distances greater than 40 Å. It was also shown that stacking interactions play an important role in the long-distance DNA radiation-induced damage repair.[3] But the investigations devoted to weak interactions occurring in the nucleic acids are still very limited. Only recently have some more results on the stacking interactions between nucleic acid bases been reported.[4−6]

In previous work,[7] we studied the competition between stacking interactions and weak H-bonding in pyrimidine dimers employing matrix isolation IR spectroscopy and *ab initio* calculations. The experimental study indicates that weakly bonded pyrimidine dimers are formed in Ar matrices. The *ab initio* calculations predict that several equilibrium geometries exist in stacked and H-bonded configurations, all with very similar energies. The final conclusion, which we based on the analysis of the experimental and theoretical data, was that the pyrimidine dimer species responsible for the experimental IR spectra of the dimer has a planar configuration.

In this present work, we undertook investigation of the intermolecular interactions in heterodimers of pyrimidine and quinone using, again, the combination of matrix isolation IR spectroscopy and theoretical *ab initio* calculations in a search for a system forming a stable stacked complex. Quinone was chosen as one of the components in the complex because it can only form weak C−H···O and C−H···N H-bond interactions with pyrimidine in the planar dimers which are presumably not strong competitors with the stacking interactions. The symmetrical quinone molecule is also desirable to use since it can only form a very limited number of different dimer conformers with pyrimidine. It should also be mentioned that quinone is a suitable model for a wide range of anthracycline antibiotics which are known to intercalate in the DNA double helix forming stacking complexes with nucleic acid bases.[8,9]

The stacking interaction as well as the C−H···N(O) H-bonded interaction are much weaker than the more conventional *N*(*O*)−*H*···N(O) H-bonding. This generates some problems in both experimental and theoretical investigations of the interactions. The spectral manifestations of weak stacked and H-bonding interactions in the matrix IR spectra are generally small. The frequency shifts of pyrimidine dimer relative to the monomer's spectra[7] are within 10 cm^{-1}. Similar small shifts can be expected in the case of quinone−pyrimidine dimer formation. A special technique of carrying out measurements allowing us to distinguish the bands of quinone−pyrimidine heterodimers from the bands of the monomers and homodimers had to be developed. The technique will be described in this work.

[†] University of Arizona.
[‡] Institute of Low Temperature Physics and Engineering National Academy of Sciences of Ukraine.
[§] University of Leuven.
[⊗] Abstract published in *Advance ACS Abstracts,* September 1, 1997.

S1089-5639(97)01444-8 CCC: $14.00

In the following sections of this paper, the data obtained from the IR spectroscopic and theoretical *ab initio* studies of the structure of quinone−pyrimidine heterodimers isolated in the argon matrix is presented. An attempt to account for the matrix effects within Onsager's reaction field methodology[10] has also been made.

2. Experimental Methods

The fill-up helium cryostat used for matrix isolation IR spectroscopy is described elsewhere.[11] The updated SPECORD IR 75 grating spectrometer was sealed and blown through with dry nitrogen during the experiment to exclude the influence of atmospheric H_2O and CO_2 vapor. The matrix samples were prepared by simultaneous deposition of the substances and the matrix gas (Ar) onto a cooled CsI substrate. The substrate temperature was maintained at 16−18 K during matrix deposition to obtain samples with optimal scattering. To prevent matrix overheating in the spectrometer beam, the samples were cooled to 12 K for spectral recording. The matrix gas was 99.99% Ar. The concentrations of the substances were controlled using a low-temperature quartz microbalance. The flow stability of the components was achieved with a stable gas pressure over the solid phase at fixed temperatures: 30 °C for quinone, 0 °C for pyrimidine, and 77 K for Ar. The densities of the substance flows were controlled with fine control valves.[12] In the case of quinone, the control valve and connecting tubes were heated up to 70 °C to avoid condensation. The IR spectra were registered in the range 4000−400 cm^{-1}. A resolution of 3 cm^{-1} was achieved in the range 4000−2500 cm^{-1}, and a resolution of 1 cm^{-1} in the range 2500−400 cm^{-1}. The absolute amounts of the substances were determined from the flow densities and deposition times. The integrated absorption coefficients may be considerably underestimated for some bands since half-widths of the bands in the matrix IR spectra are much smaller then the spread function width of the spectrometer. The spectra of quinone were scaled by assuming the surface density of quinone in the samples to be 3.0×10^{-5} g/cm^2, and the spectra of pyrimidine were scaled by assuming a surface density of pyrimidine to be 3.6×10^{-5} g/cm^2.

3. Experimental Results

The main aim of these experiments is identification of bands of quinone−pyrimidine dimer in the matrix IR spectra. To accomplish this we had to prepare a sample with a maximum quantity of heterodimers and to learn how to separate bands arising from heterodimers from bands due to monomers and homodimers.

Gradually increasing the concentration of the studied substance in the matrix is a common method to maximize the concentration of dimers in the matrix. Matrix annealing can also lead to an additional increase in dimer concentration. However, a point is reached beyond which further increases in substance concentration begin to yield disordered complexes in the matrix whose bands disguise those of the dimers. To characterize this process, we undertook an investigation of the influence of the amount of substance on the concentrations of monomers, dimers, and larger complexes in the matrix.[13] The unique low-temperature quartz microbalance[11] was used which allows measurement of the gaseous flows of both the substance studied and the inert Ar gas to allow precise and accurate determination of the concentration of the substance in the matrix.

Firstly, we investigated the dependence between the total concentration of a substance in the matrix and the concentration of the dimers. In this investigation we chose phenol as the model compound because its molecules have approximately the same size as the molecules of pyrimidine and quinone. We assumed that at the same concentration of phenol, quinone, and pyrimidine in the matrix, the ratios of monomers, dimers, and higher associates for each of these compounds are very similar. Phenol is a convenient model compound because the phenol dimers have a strong intermolecular O−H···*O* H-bond which enables its easy identification in the matrix IR spectra based primarly on the shift of the band due to the OH stretching vibration. In this initial calibration experiment samples with the following concentrations were investigated: 1:1000, 1:500, 1:250, 1:125, 1:60, and 1:30 (solute:matrix). At the 1:1000 concentration of phenol to argon, 95% of phenol molecules were found to exist as monomers and 5% as dimers. At higher solute concentrations up to the concentration of 1:250, the concentration of the dimers increases to 16% when measured immediately after matrix deposition and to 25% after matrix annealing. At the 1:125 concentration the amount of dimers in the sample was the same as that at the 1:250 concentration, and further increases of the concentration resulted in a decrease of the concentration of the dimers due to preferential formation of larger disordered complexes. Thus, at the concentrations from 1:250 through 1:125 the dimer percentage is at a maximum of approximately 25%. When the concentration increases from 1:250 to 1:125 the percentage of larger complexes increases significantly, from ≈5% to ≈37%. Therefore, the ratio of phenol to matrix of 1:250 is the optimal concentration for investigation of dimers. This ratio was presumed to be optimal for the investigation of quinone−pyrimidine dimers as well.

To distinguish the bands of quinone−pyrimidine heterodimers, we had to separate them from the bands from pyrimidine and quinone monomers as well as from the bands from pyrimidine and quinone dimers. The separation of the heterodimer spectrum from the spectra of the monomers and homodimers was accomplished by comparison of data obtained from a total of six mixed and unmixed quinone and pyrimidine samples. The first two samples contained ratios of quinone: pyrimidine:argon of 4:1:1000 and 1:4:1000. In the first sample the following systems were present: (i) pyrimidine monomers, (ii) quinone monomers, (iii) quinone dimers and larger quinone associates, and (iv) quinone−pyrimidine dimers. In the second sample the following systems were present: (i) quinone monomers, (ii) pyrimidine monomers, (iii) pyrimidine dimers and larger pyrimidine associates, (iv) quinone−pyrimidine dimers. The remaining four samples did not contain mixed quinone and pyrimidine: pyrimidine:Ar (1:1000), pyrimidine: Ar (1:250), quinone:Ar (1:1000), and quinone:Ar (1:250).

The vibrational bands arising primarily from the pyrimidine molecule within the pyrimidine−quinone dimer were identified by comparing the spectrum of the quinone:pyrimidine:Ar (4: 1:1000) sample with the spectra of the pyrimidine monomer (1:1000) sample and the quinone monomer (1:1000) and dimer (1:250) samples. Similarly, the vibrational bands arising primarily from the quinone molecule within the pyrimidine− quinone dimer were identified by comparing the spectrum of the quinone:pyrimidine:Ar (1:4:1000) sample with the spectra of the quinone monomer (1:1000) sample and the pyrimidine monomer (1:1000) and dimer (1:250) samples. The frequencies of pyrimidine and quinone monomers as well their shifts resulting from the formation of the homo- and heterodimers are given in Tables 1 and 2. The spectral regions containing the bands of the quinone−pyrimidine dimer are shown in Figures 1 and 2.

A total of nine vibrational bands attributed to the pyrimidine− quinone dimer were found. Five of them arise from primarily the pyrimidine portion of the heterodimer, and four from

TABLE 1: Observed IR Frequencies (cm^{-1}) and Intensities (km mol^{-1}) of Pyrimidine Monomer and Shifts (cm^{-1}) of the Pyrimidine Bands in the Complexes Pyrimidine−Pyrimidine and Pyrimidine−Quinone Isolated in Argon Matrices

pyrimidine		pyrimidine−pyrimidine	pyrimidine−quinone
frequency	intensity	shift	shift
3140	2.0	0	0
3090	1.8	0	0
3058	1.8	0	0
3053	4.4	0	0
3042	8.4	0	0
3019	1.6	0	0
3008	0.8	0	0
2963	1.4	0	0
2921	2.5	0	0
1570	28	+3	+2
1567	18	0	0
1465	5.5	0	0
1400	29	+6.5	+5
1223	5.2	+4.5	+4
1157	2.6	0	0
1074	1.6	0	*a*
1071	1.3	0	*a*
990	2.0	0	0
804	3.1	*b*	*b*
719	21	+4	+3
687	1.5	0	0
621	6	+1.5	+1

[a] The band of pyrimidine is eclipsed by quinone one. [b] The monomer band is weak; we suspect presence of shifted bands of associates in the spectrum, but due to low intensity we cannot define their accurate location.

TABLE 2: Observed IR Frequencies (cm^{-1}) and Intensities (km mol^{-1}) of Quinone Monomer and Shifts (cm^{-1}) of the Quinone Bands in the Complexes Quinone−Quinone and Quinone−Pyrimidine in Argon Matrices

quinone		quinone−quinone	quinone−pyrimidine
frequency	intensity	shift	shift
1755	3.5	0	0
1707	5.3	0	0
1682	25	0	0
1672	70	0	0
1670	40	0	0
1659	52	+2	+2.5
1640	2.9	0	0
1596	9	*a*	*a*
1357	4.7	0	0
1353	2	0	0
1301	3	+2.5	+4
1066	17	+4.5	*b*
942	9	0	0
886	50	+6.5	+6
503	2.9	0	0
407	18	+3	+2

[a] The monomer band is weak; we suspect the presence of shifted bands of associates in the spectrum, but due to low intensity we cannot define their accurate location. [b] The band of quinone is eclipsed by pyrimidine one.

primarily the quinone portion. The observed bands occur in a very wide spectral range of 1700 to 400 cm^{-1}. It is notable that half-widths of the heterodimer bands only slightly exceed the half-widths of the bands of the quinone and pyrimidine monomers. This minimal broadening means that the quinone−pyrimidine dimers have a well-defined structure. The largest frequency difference between the dimer bands and the bands of the corresponding monomers does not exceed 10 cm^{-1}, which is similar to the previously studied pyrimidine dimer system.[7]

In two spectral regions, the bands of the quinone−pyrimidine dimers were not observed. The CH stretching vibrations of quinone are very weak and were not identified in the low

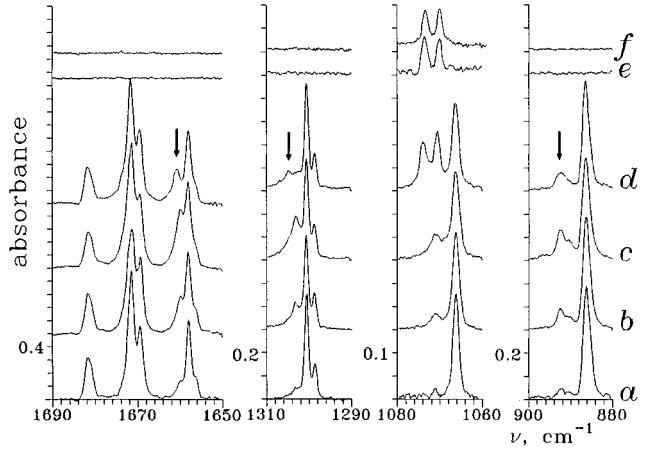

Figure 1. IR spectra of quinone ($T = 12$ K) at $M = 1{:}1000$ (a), 1:250 (b), 1:125 (c); quinone−pyrimidine IR spectrum at $M = 1{:}4{:}1000$ (d); IR spectra of pyrimidine at $M = 1{:}1000$ (e), 1:250 (f). The arrow marks the bands of the quinone−pyrimidine dimers.

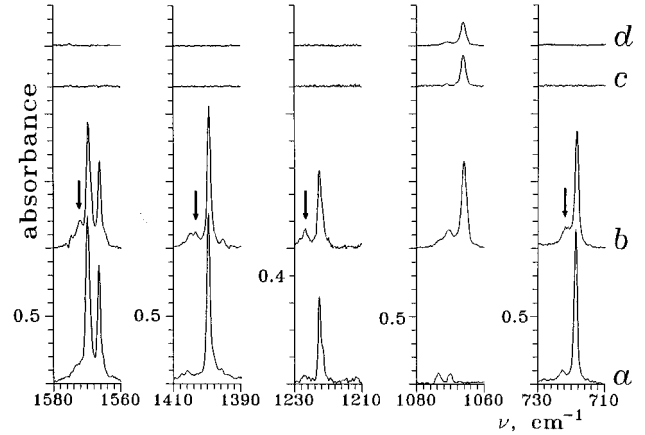

Figure 2. IR spectrum of pyrimidine ($T = 12$ K) at $M = 1{:}1000$ (a); pyrimidine−quinone IR spectrum at $M = 1{:}4{:}1000$ (b); IR spectra of quinone at $M = 1{:}1000$ (c), 1:250 (d). The arrow marks the bands of the quinone−pyrimidine dimers.

quinone concentration (1:1000) spectrum. In the 1070−1060 cm^{-1} region, the 1066 cm^{-1} pyrimidine band and 1074, 1071 cm^{-1} quinone bands eclipse those of the heterodimer.

Until now spectral manifestations of weak intermolecular interactions have not been studied in detail, and the empirical analysis of the quinone−pyrimidine bands does not provide sufficient information to determine the heterodimer structure. The lack of previous empirical classification of quinone−pyrimidine heterodimer necessitated the present comparison of matrix isolation IR spectra with *ab initio* determined structures and vibrational spectra. The information obtained from comparison of the experimental spectra with the frequency shifts theoretically predicted for different heterodimer equilibrium geometries allows assignment of the structure of the dimer.

4. Theoretical Method

The self-consistent field (SCF) level of theory with the 6-31++G** basis set was initially applied to find quinone−pyrimidine heterodimer equilibrium geometries. This method predicted two planar equilibrium dimer geometries, but all attempts to find a stacked equilibrium geometry at this level of theory failed and always led to planar configurations. This was not an unexpected result since stacked geometries occur due to stabilization by dispersion forces, requiring the inclusion of electron correlation in the calculations. Additionally, attempts to find the stacked pyrimidine dimer by employing the density

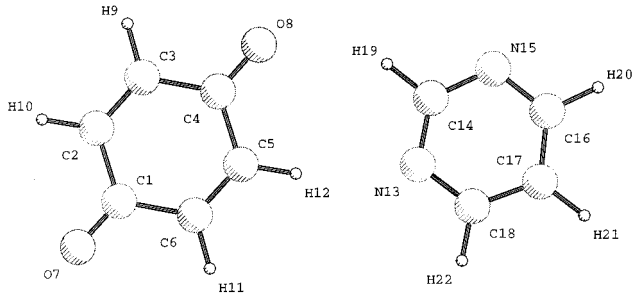

Figure 3. Equilibrium PlanarA geometry calculated at the MP2/6-31+G* level.

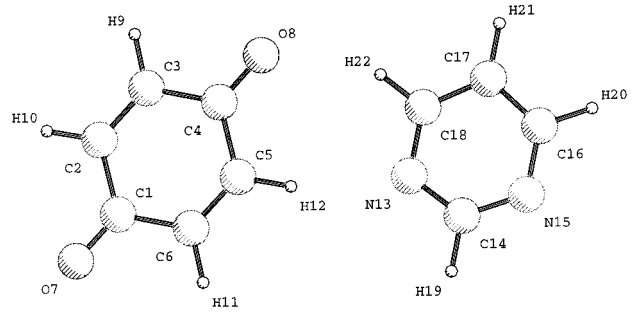

Figure 4. Equilibrium PlanarB geometry calculated at the MP2/6-31+G* level.

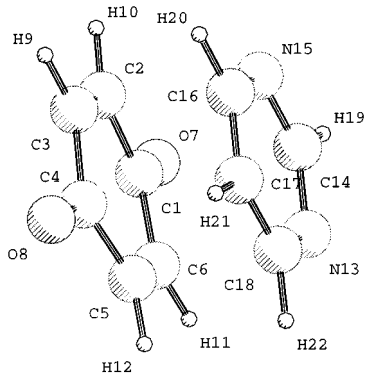

Figure 5. Equilibrium Stacked geometry calculated at the MP2/6-31+G* level.

functional theory (DFT) method also failed and led to planar geometries. However, optimizations of the dimers performed by applying the Møller−Plesset second-order perturbation theory (MBPT(2)=MP2)[14] with the 6-31 type Gaussian basis set augmented with diffuse and polarization functions on heavy atoms (the 6-31+G* basis set) resulted in the discovery of a stable stacked conformer. Three stable structures of the quinone−pyrimidine dimers were found overall in the calculations. Two of the dimers are planar complexes that we label PlanarA and PlanarB, and the third is a Stacked complex. The equilibrium geometry structures are depicted in Figures 3−5. Among the SCF, DFT, and MP2 methods used to characterize stacking interactions,[4,5] only the latter method yielded a stable stacked dimer, the other two methods did not converge to such a structure. The MP2 method is the lowest level of theory capable of accounting for all major interaction effects in H-bonded systems and stacked aromatic rings. These effects include the electrostatic, induction, charge transfer, exchange, and, particularly, dispersion interactions.

The interaction energies in the dimers were estimated with an account of basis set superposition error (BSSE) by the counterpoise method proposed by Boys and Bernardi.[15] This method involves a single calculation for the dimer and two calculations for the monomers with the basis set of the dimer. The MP2/6-31+G* calculations were done to determine the energy of the monomers with the dimer basis sets for all three dimers. In the calculations on monomers, the monomer equilibrium geometries were used. The BSSE-corrected interactions energies were calculated for each dimer as the difference of the dimer energy and monomer energies calculated with the dimer basis set.

The total energies, interaction energies, dipole moments, zero-point energies (ZPE), and relative energies, as well as the BSSE corrections and corrected interaction energies, are summarized in Table 3. The ZPE contributions were determined from the harmonic frequencies calculated from analytical second derivatives of the Hartree−Fock energies. Limitations of the computer systems available to us precluded application of the MP2 method to the determination of harmonic frequencies at this level of theory.

The SCF frequency analysis for the dimers was carried out in the following way:

(1) The geometries of three dimers were fully optimized at the MP2/6-31+G* level.

(2) The intramolecular coordinates (the internal coordinates of the monomers) were then reoptimized at the SCF/6-31++G** level while the six intermolecular parameters (the internal coordinates describing the relative orientation of the pyrimidine and quinone rings toward each other) were frozen.

(3) Finally, SCF/6-31++G** harmonic vibrational frequencies were calculated.

The resultant SCF frequencies corresponding to intermolecular vibrational modes are suspect since the intermolecular parameters were optimized at the MP2 level. In fact, this method produced an imaginary frequency for the lowest vibrational mode for each dimer. However, this did not produce any practical difficulties for our study since the experimental procedure did not probe the low-frequency region. To analyze the matrix IR spectra of pyrimidine and quinone monomers, the harmonic frequencies and intensities were calculated at the SCF/6-31++G** level for the monomer geometries fully optimized at this level of theory.

Additionally, MP2/6-31++G** calculations for the three dimers were carried out using geometries with intermolecular parameters optimized at the MP2/6-31+G* level and intramolecular parameters optimized at SCF/6-31++G** level. The BSSE corrections at MP2/6-31++G** level were determined in the same way as described before for the MP2/6-31+G* calculations. The energies, interaction energies, relative energies, and BSSE-corrected interaction energies calculated at the MP2/6-31++G** level are listed in Table 4.

All calculations presented in this work were performed using the Gaussian92 software package.[16]

5. Quinone−Pyrimidine Dimer Energies and Structure

As mentioned before, two planar structures stabilized by C−H···N and C−H···O H-bonds (Figures 3 and 4) and a single stacked structure stabilized by dispersion forces (Figure 5) were found for the quinone−pyrimidine complex. The main difference between the two planar quinone−pyrimidine configurations (PlanarA and PlanarB) is in which pyrimidine carbon atom acts as the H-bond proton donor. In the PlanarA dimer it is C_2 (labeled 14 in the figures), and in the PlanarB dimer it is C_4 (labeled 18 in the figures). One can identify two major factors which contribute to the stabilization of the planar complexes. The first is the higher acidity of the C_2 atom than that of the C_4 atom due to its closer location to the two nitrogen atoms in the ring. Due to this effect the C−H···O H-bond in the PlanarA dimer should be stronger than the one in the PlanarB dimer.

TABLE 3: Energies (au), Relative Stabilities (kJ mol^{-1}), Interaction Energies (kJ mol^{-1}), Dipole Moments (D), Scaled (0.9) Zero Point Vibrational Energies Taken from HF/6-31++G Frequency Calculations (au), Total Energies Including the Zero-Point Vibrational Energy (au) and Relative Stabilities Including the Zero-Point Vibrational Energy (kJ mol^{-1}) of the Three Possible Complexes between Pyrimidine and Quinone[a]**

	PlanarA	PlanarB	Stacked
MP2/6-31+G*	−643.886 484 9	−643.887 841 7	−643.892 108 5
Δ*E*(MP2)	14.76	11.20	0.0
IE(MP2)	−21.80	−25.36	−36.56
ZPE[b]	0.157 716 8	0.157 731 2	0.158 161 5
MP2+ZPE	−643.728 768 1	−643.730 110 5	−643.733 947 0
Δ*E*(MP2+ZPE)	13.60	10.07	0.0
dipole moment	2.73	2.64	3.13
	Energy of Pyrimidine Monomer		
MP2/6-31+G*		−263.5264625	
	Energy of Quinone Monomer		
MP2/6-31+G*		−380.3517188	
	Pyrimidine with Ghost Functions		
MP2/6-31+G*	−263.528 000 4	−263.527 956 3	−263.530 369 2
	Quinone with Ghost Functions		
MP2/6-31+G*	−380.352 923 0	−380.353 030 0	−380.356 170 6
BSSE	0.002 742 1	0.002 805 0	0.008 358 5
MP2+BSSE	−643.883 742 8	−643.885 036 7	−643.883 751 0
Δ*E*(MP2+BSSE)	3.40	0.00	3.37
IE(BSSE-corrected) at MP2 level	−14.59	−17.99	−14.62
MP2+BSSE+ZPE	−643.726 026 0	−643.727 305 5	−643.725 589 5
Δ*E*(MP2+BSSE+ZPE)	3.36	0.00	4.50

[a] Values are taken from the full optimization of the complexes at the MP2/6-31+G* level. [b] Calculated at HF/6-31++G** level of theory for the complexes with intermolecular parameters optimized at MP2/6-31+G* level of theory and intramolecular parameters optimized at HF/6-31++G** level of theory.

TABLE 4: Energies (au), Scaled Zero Point Vibrational Energies (au), Relative Stabilities (kJ mol^{-1}), Interaction Energies (IE, kJ mol^{-1}), and Interaction Energies Corrected for the Basis Set Superposition Error (BSSE, kJ mol^{-1}) for the Three Pyrimidine:Quinone Complexes

method	PlanarA	PlanarB	Stacked
Hartree−Fock[a]	−641.966 216 0	−641.967 367 5	−641.959 428 0
MP2[b]	−643.937 773 1	−643.939 083 5	−643.941 637 7
Δ*E*(MP2)	10.15	6.71	0.00
IE at HF level	−10.52	−13.55	+7.30
IE at MP2 level	−22.87	−26.31	−33.02
ZPE[c]	0.157 716 8	0.157 731 2	0.158 161 5
MP2+ZPE	−643.780 056 3	−643.781 352 3	−643.783 476 2
Δ*E*(MP2+ZPE)	8.98	5.58	0.00
IE at HF level + ZPE	+13.17	+10.19	+32.16
IE at MP2 level + ZPE	+0.82	−2.58	−8.15
	Pyrimidine with Ghost Functions		
HF	−262.708 481 8	−262.708 423 7	−262.708 691 7
MP2	−263.556 043 5	−263.555 932 4	−263.557 734 2
	Quinone with Ghost Functions		
HF	−379.254 547 3	−379.254 564 6	−379.255 516 8
MP2	−380.375 984 8	−380.376 089 2	−380.379 029 5
BSSE at HF level	0.000 821 4	0.000 780 6	0.002 000 8
BSSE at MP2 level	0.002 968 0	0.002 961 3	0.007 703 4
MP2+BSSE	−643.934 805 1	−643.936 122 2	−643.933 934 3
Δ*E*(MP2+BSSE)	3.46	0.00	5.75
IE(BSSE-corrected) at HF level	−8.36	−11.50	+12.55
IE(BSSE-corrected) at MP2 level	−15.08	−18.54	−12.79
MP2+BSSE+ZPE	−643.777 088 3	−643.778 391 0	−643.775 772 8
Δ*E*(MP2+BSSE+ZPE)	3.42	0.00	6.87

[a] Intramolecular parameters were reoptimized at the HF/6-31++G** level of theory after full optimization at the MP2/6-31+G* level of theory. [b] Single point calculation at the MP2/6-31G++G** level of theory for the complexes with intermolecular parameters optimized at the MP2/6-31+G* level of theory and intramolecular parameters optimized at the HF/6-31++G** level of theory. [c] Calculated at the HF/6-31++G** level of theory for the complexes with intermolecular parameters optimized at the MP2/6-31+G* level of theory and intramolecular parameters optimized at the HF/6-31++G** level of theory.

The second effect is due to a shorter distance between the two negatively charged pyrimidine nitrogen atoms and the quinone oxygen atom in the PlanarA dimer than that in the PlanarB dimer. This effect should weaken the intermolecular interaction in the PlanarA dimer. The competiton between these two factors decides the relative stability of the quinone−pyrimidine planar dimers.

The energies of the dimers fully optimized at MP2/6-31+G* level are listed in Table 3. If the BSSE corrections are not accounted for, the Stacked dimer with an interaction energy of −36.56 kJ mol^{-1} is predicted to be more stable than the planar dimers. The relative energies of the PlanarA and PlanarB dimers calculated with respect to the Stacked dimer are 14.76 and 11.20 kJ mol^{-1}, respectively. Account of the zero-point

vibration energies calculated at the SCF/6-31++G** level and scaled by the factor of 0.9 slightly decreases the energy gap between the planar and stacked dimers. With this contribution, the corresponding relative energies are 13.60 and 10.07 kJ mol^{-1}, respectively.

After accounting for the BSSE, the stability order of the dimers changes. The values of the BSSE calculated by the counterpoise method are 21.94 kJ mol^{-1} for the Stacked dimer and only 7.20 and 7.36 kJ mol^{-1} for the PlanarA and PlanarB dimers, respectively. Very similar results were obtained earlier for planar and stacked pyrimidine homodimers.[7] Most likely, the BSSE calculated for the Stacked conformer is greater due to the closer proximity of the ghost functions in the calculation of the monomer with the dimer basis set. Thus, the calculations at the MP2/6-31+G* level with the BSSE corrections predict that the PlanarB dimer is the most stable form, although the energy differences between all the dimers are rather small (less than 5 kJ mol^{-1}). The BSSE-corrected interaction energies are −14.59, −17.99, and −14.62 kJ mol^{-1} for the PlanarA, PlanarB, and Stacked dimers, respectively.

Single-point calculations at the MP2/6-31++G** level were carried out for the three dimers with intermolecular parameters optimized at the MP2/6-31+G* level and intramolecular parameters optimized at the SCF/6-31++G** level. (These geometries were also used in the harmonic frequency calculations, as described above.) The MP2/6-31++G**//MP2/6-31+G*(inter) and SCF/6-31++G**(intra) results are presented in Table 4. We may expect that the augmentation of the 6-31+G* basis set with diffuse and polarization functions on hydrogens will preferably increase the stability of the H-bonded planar dimers. In fact, as seen in Table 4, the energy difference between PlanarA and PlanarB dimers does not change significantly, although the energy difference between planar dimers and the stacked dimer decreases by 4.5 kJ mol^{-1} (non-BSSE-corrected energies). The comparison of the BSSE-corrected MP2/6-31+G* and MP2/6-31++G** relative energies shows that the enlargement of the basis set leads to a decreased BSSE for the Stacked dimer by 1.72 kJ mol^{-1} and to an increased BSSE for the PlanarA and PlanarB dimers by 0.59 and 0.41 kJ mol^{-1}, respectively. The MP2/6-31++G** results with BSSE corrections predict that the PlanarB dimer is the most stable form and that there are only small energy differences between all the dimers, which is similar to the MP2/6-31+G* results. This could possibly mean that both planar and stacked dimers coexist in the argon matrices.

As was mentioned before, the SCF/6-31++G** structure calculations did not converge to a stacked geometry of the quinone−pyrimidine complex. The inability of the SCF method to predict the stacked structure of the complex is reflected in the positive interaction energy of the Stacked quinone−pyrimidine dimer obtained when this method was applied to optimize the intramolecular parameters of this dimer while the intermolecular parameters were frozen at values obtained at the MP2/6-31+G* level (Table 4). However, for the two planar H-bonded dimers, the SCF method yielded energy differences comparable to those from the MP2 calculations (see Table 5). The data presented in Table 5 for the two planar geometries differs only in how the intermolecular parameter values were obtained. The energies listed in Table 4 are from geometries in which the intermolecular parameters were calculated at the MP2/6-31+G* level and the intramolecular parameters were calculated at the SCF/6-31++G** level. The energies listed in Table 5 are from geometries in which the both the inter- and intramolecular geometries were calculated at the SCF/6-31++G** level. Comparison of the results for the two planar heterodimers in Tables 4 and 5 reveals the performance of the SCF method in predicting the structures and energies of complexes stabilized by weak C−H···N(O) H-bonds. The comparison of the SCF energies of the two planar dimers listed in Tables 4 and 5 shows that in both cases the PlanarB dimer is predicted to be more stable. The relative energies of the dimers are 3.03 and 3.09 kJ mol^{-1}, respectively. Single-point calculations were also performed for the two planar heterodimers at the MP2/6-31++G**//SCF/6-31++G** level of theory. Again, very similar values of the relative energies of the PlanarA and PlanarB quinone−pyrimidine dimers with intermolecular parameters optimized at MP2/6-31+G* and SCF/6-31++G** levels were found. They are 3.44 and 3.47 kJ mol^{-1}, respectively.

TABLE 5: Energies (au) and Relative Stabilities (kJ mol^{-1}) of Two H-Bonded Pyrimidine:Quinone Complexes Optimized at the HF/6-31++G Level of Theory**

	PlanarA	PlanarB
HF/6-31++G**	−641.966 648 8	−641.967 825 6
MP2/6-31++G**//HF/6-31++G**	−643.937 279 2	−643.938 613 9
ΔE(HF)	3.09	0.00
ΔE(MP2)	3.50	0.00
IE at HF level	−11.66	−14.75
IE at MP2 level	−21.58	−25.08
ZPE at HF level	0.157 716 8	0.157 731 2
MP2+ZPE	−643.779 562 4	−643.780 882 7
ΔE(MP2 + ZPE)	3.47	0.00
Energies of Pyrimidine Monomer		
HF/6-31++G**	−262.707 966 3	
MP2/6-31++G**//HF/6-31++G**	−263.554 392 0	
ZPE at HF level	0.066 245 0	
Energies of Quinone Monomer		
HF/6-31++G**	−379.254 241 4	
MP2/6-31++G**//HF6-31++G**	−380.374 668 3	
ZPE at HF level	0.082 446 3	

In conclusion, different theoretical methods have been applied to determine the structure and relative stabilities of planar and stacked quinone−pyrimidine dimers. The PlanarB dimer was found to be the most stable form, but the energy differences between all the dimers are too small to preclude their possible formation in the argon matrices. The question of which dimer is responsible for the experimentally observed phenomena can only be answered based on the comparison of the theoretically predicted and experimentally observed spectral features.

6. Vibrational Spectra of the Quinone−Pyrimidine Dimer

There were no large changes observed in the experimental IR spectra which occurred due to formation of the quinone−pyrimidine dimer. The absence of stronger spectral manifestations of quinone−pyrimidine heterodimer formation results from the inherent weakness of the forces binding the dimer. As is seen in Tables 1 and 2, none of the observed shifts of pyrimidine and quinone monomer vibrations due to the formation of the complex exceeds 6 cm^{-1}. Shifts of this magnitude preclude the determination of the structure of the quinone−pyrimidine complex based only on empirical analysis. The quantum mechanical calculations performed in this work provide additional assistance in assigning the dimer structures. The observed shifts of the monomer bands and shifts calculated for two types of dimers—*Planar B* and Stacked—are compared. A determination is made as to which of the calculated spectra match better to the experimental data.

The observed infrared frequencies and intensities of the monomers are presented in Tables 1 (pyrimidine) and 2

TABLE 6: Calculated Frequencies (cm^{-1}) and IR Intensities (km mol^{-1}) of Quinone and Pyrimidine Monomers and Frequencies, Intensities, and Band Shifts on Dimer Formation of PlanarB and Stacked Quinone−Pyrimidine Complexes

quinone		pyrimidine		PlanarB			Stacked		
ν	I	ν	I	ν	I	shift	ν	I	shift
3052	0.0			3050	2.4	−2	3059	0.3	+7
		3054	6.1	3057	10.4	+3	3058	5.8	+4
3050	3.0			3042	4.6	−8	3055	1.0	+5
		3042	21.7	3041	1.3	−1	3040	15.8	−2
3033	0.7			3033	0.5	0	3038	0.7	+4
3033	0.0			3012	71.6	−21	3037	0.5	+3
		3023	24.8	3036	19.0	+13	3025	21.8	+2
		3018	10.7	3021	21.6	+3	3021	11.0	+3
1801	0.0			1797	27.0	−4	1797	6.2	−4
1781	775.2			1773	830.3	−8	1775	762.9	−6
1659	0.0			1657	0.9	−2	1659	0.2	0
1640	9.1			1638	12.9	−2	1639	10.3	−1
		1611	115.4	1616	174.6	+5	1613	127.3	+2
		1611	130.1	1607	84.4	−4	1609	73.5	−2
		1468	18.7	1469	33.6	+1	1469	18.7	+1
		1409	82.0	1414	84.9	+5	1409	70.4	0
1375	0.0			1385	6.7	+10	1374	0.2	−1
		1358	1.22	1365	0.1	+7	1358	1.0	0
1353	3.5			1361	3.6	+8	1352	3.4	−1
1288	103.9			1293	107.8	+5	1287	77.2	0
		1216	12.8	1223	29.9	+7	1216	6.1	0
1206	0.0			1212	0.2	+6	1205	0.1	−1
1137	0.0			1150	0.5	+13	1137	0.6	0
		1129	0.4	1132	2.8	+3	1129	0.1	0
		1091	12.6	1088	12.2	−3	1089	12.4	−2
1057	43.5			1067	39.9	+10	1057	35.1	0
		1045	2.2	1050	2.2	+5	1049	2.5	+4
		1042	2.0	1044	8.2	+2	1044	0.2	+2
		1032	0.1	1043	0.0	+11	1041	0.3	+9
		1011	0.0	1023	0.0	+12	1014	0.0	+3
1003	0.0			1017	0.5	+14	1013	0.2	+10
988	0.0			992	0.0	+4	1007	0.2	+19
		991	4.7	992	5.7	+1	993	8.1	+2
		982	1.0	985	0.8	+3	986	0.8	+4
924	15.9			924	25.2	0	926	14.8	+2
885	125.0			890	119.4	+5	890	130.1	+5
		813	10.9	818	12.4	+5	812	6.9	−1
748	0.0			755	0.7	+7	773	1.9	+25
742	0.0			739	1.0	−3	747	2.7	+5
738	0.0			729	0.9	−9	739	0.5	+1
726	0.3			727	0.5	+1	726	0.1	0
		703	59.6	705	54.8	+2	707	66.5	+4
		674	3.7	675	2.0	+1	674	2.0	0
		614	12.5	616	24.9	+2	614	12.1	0
582	0.0			584	0.1	+2	582	0.0	0
502	2.8			511	1.9	+8	510	1.5	+8
441	0.0			444	1.2	+3	442	0.	+1
434	0.0			436	0.6	+2	433	0.6	−1
		412	0.0	413	0.0	+1	414	0.6	+2
404	36.8			407	46.8	+3	404	29.9	0
		369	3.5	369	2.9	0	375	4.6	+6
333	0.0			326	0.0	−7	342	0.2	+9
198	0.0			162	0.4		234	2.1	
82	18.6			81	17.6		108	24.5	
				73	0.0		91	1.8	
				55	2.0		69	0.8	
				44	2.4		64	1.1	
				42	0.3		49	0.5	
				27	0.0		35	0.3	
				15	0.6		20	0.9	

(quinone), and the calculated data for both monomers are presented in Table 6. Very good agreement between the calculated and observed frequencies of the monomers is observed for almost all vibrations. The average difference is 17 cm^{-1} for pyrimidine and 24 cm^{-1} for quinone. One can note that in some spectral regions the number of observed bands exceeds the number of calculated bands. This observation is particularly applicable to the region of the C−H stretching vibrations in the pyrimidine IR spectrum and to the region of the C═O stretching vibrations in the quinone IR spectrum. We suspect that additional lines in the experimental spectra in these regions may be caused by matrix splitting and/or Fermi resonances.

In the calculations, an attempt was made to account for the effects of BSSE on the calculated harmonic frequencies of the monomers. Since BSSE was found to significantly affect the relative stabilities of the planar and stacked dimers, it is reasonable to expect that it also affects the calculated frequency shifts. In correcting for BSSE, the frequencies of the quinone and pyrimidine monomers were calculated with the basis sets of the PlanarB and Stacked dimers. Prior to these calculations, the geometries of both monomers were optimized in the dimer basis sets with the coordinates defining the positions of the ghost basis functions frozen. Next, the force constant matrix was analytically determined (this includes only the second derivatives of the energy with respect to the displacements of the atoms of the monomer, not the ghost atoms) and mass weighted. Then, its eigenvalues were found, which are proportional to the squared normal-mode frequencies. However, no difference between non-BSSE-corrected and BSSE-corrected frequencies greater than 1 cm^{-1} was found for any of the monomers.

The results of harmonic frequency calculations of the most stable planar dimer, PlanarB, and the Stacked dimer are listed in Table 6 along with the calculated shifts of monomer frequencies due to the dimer formation. To better compare the observed and calculated frequency shifts, we picked out vibrations which met two conditions: they had to have higher predicted intensities, and their calculated shifts due to the dimer formation had to exceed at least 2 cm^{-1}. The data for these selected frequencies as well as experimentally observed bands of the quinone−pyrimidine dimer are listed in Table 7. The results of the potential energy distribution analysis of the pyrimidine and quinone monomers and PlanarB and Stacked dimers are summarized in Tables 1S−4S.

The following groups of frequencies were made to simplify the comparison of the calculated and observed frequency shifts:

(1) For frequency 886 cm^{-1}, the calculations predict nearly identical shifts for PlanarB (+5.4 cm^{-1}) and Stacked (+5.2 cm^{-1}) dimers, and the shifts are in agreement with the experimental one (+6 cm^{-1}). Unfortunately, despite the agreement between calculated and experimental shifts, this datum does not allow us to determine which type of dimer is responsible for the observed shift.

(2) For three bands of the pyrimidine monomer (1570, 719, and 621 cm^{-1}) the observed shifts are +2, +3, and +1 cm^{-1}, respectively. The corresponding shifts predicted for PlanarB and Stacked dimers are not identical but close enough (Table 7) so that a definite assignment of the observed bands to a particular dimer is again not possible.

(3) A new band at 1661.5 cm^{-1}, assigned to a quinone molecular vibration in the quinone−pyrimidine dimer spectrum, appears in the C═O stretching region (1690−1650 cm^{-1}, Figure 1). One can see that a few bands of the quinone monomer also can be found in this region (Table 2, Figure 1). Although initially the 1661.5 cm^{-1} band of the dimer was correlated to the 1659 cm^{-1} band of the quinone monomer (with a corresponding shift of +2.5 cm^{-1}), the band can also be correlated to the monomer band which appears at 1670 cm^{-1} (with a corresponding shift of −8.5 cm^{-1}). The latter assignment is in better agreement with the calculated shifts which are −7.6 cm^{-1} for the PlanarB dimer and −5.3 cm^{-1} for the Stacked dimer (Table 7).

TABLE 7: Comparison of Calculated and Observed Band Shifts for PlanarB and Stacked Quinone−Pyrimidine Dimers[a]

calculated									observed		
monomer			PlanarB			Stacked					
M[b]	ν	I	ν	I	shift	ν	I	shift	M[b]	ν	shift
q	3033.1	0.0	3011.5	71.6	−21.6	3036.5	0.5	+3.4			
p	3022.6	24.8	3035.8	19.0	+13.2	3024.6	21.8	+2.0			*c*
q	1780.6	775.2	1773.0	830.3	−7.6	1775.3	762.9	−5.3	q	1659	+2.5[d]
p	1611.4	115.4	1615.5	174.6	+4.1	1612.6	127.3	+1.2	p	1570	+2
p	1611.4	130.1	1607.1	84.4	−4.3	1609.0	73.5	−2.4			
p	1408.7	82.0	1414.1	84.9	+5.4	1408.9	70.4	+0.2	p	1400	+5
q	1375.0	0.0	1384.8	6.7	+9.8	1373.6	0.1	−1.4			
q	1353.0	3.5	1361.1	3.6	+8.1	1352.2	3.4	−0.8			
q	1287.9	103.9	1293.1	107.8	+5.2	1286.8	77.	−1.1	q	1301	+4
p	1216.2	12.8	1222.8	29.9	+6.7	1216.4	6.1	+0.2	p	1223	+4
p	1090.6	12.6	1087.6	12.2	−3.0	1089.0	12.4	−1.6	p	1074/1071	
q	1057.1	43.5	1066.6	39.9	+9.5	1057.3	35.1	+0.2	q	1060	
p	1045.2	2.2	1049.6	2.2	+4.4	1048.4	2.5	+3.2			
p	1042.1	2.0	1043.5	8.2	+1.4	1043.8	0.2	+1.7			
q	884.5	125.0	889.9	119.4	+5.4	889.7	130.1	+5.2	q	886	+6
p	812.6	10.9	817.5	12.4	+4.9	812.2	6.9	−0.4	p	804	*e*
p	703.0	59.6	704.8	54.8	+1.8	707.0	66.5	+4.0	p	719	+3
p	613.9	12.5	616.0	24.9	+2.1	614.0	12.1	+0.1	p	621	+1
q	404.0	36.8	406.7	46.8	+2.7	404.4	29.9	+0.4	q	407	+2

[a] Additional significant figures are included to increase the accuracy of the calculated frequency shifts. [b] q = quinone, p = pyrimidine. [c] The corresponding observed band of pyrimidine monomer (3019 cm^{-1}) is very weak (Table 1). [d] The observed band is split in the quinone IR spectra. The listed shift of +2.5 cm^{-1} was calculated with respect to the nearest monomer band. See also comment in the text. [e] We suspect the presence of the dimer band, but the corresponding monomer band is too weak to define the accurate value of the shift.

(4) For bands 1400 and 1223 cm^{-1} of the pyrimidine monomer and 1301 and 404 cm^{-1} of the quinone monomer, the observed shifts are +5, +4, +4, and +2 cm^{-1}, respectively. For this group of frequencies, the calculations predict different shifts for the PlanarB and Stacked dimers. The shifts calculated for the PlanarB dimer are clearly in better agreement with experimental shifts than for the Stacked dimer. This is the most important group of frequencies because their analysis allows us to identify the structure of the quinone−pyrimidine dimer formed in Ar matrices. As seen from Table 7, these shifts correlate well with the calculated shifts for the PlanarB dimer, which are +5.4, +6.7, +5.2, and +2.7 cm^{-1}, respectively. At the same time, the shifts of the corresponding bands of the Stacked dimer are predicted to be +0.2, +0.2, −1.1, and +0.4 cm^{-1}, which clearly do not match the experimental data. On the basis of this analysis, we assign the planar dimer configuration as the one responsible for the experimentally observed shifts.

As seen in Table 7, the calculations also predict shifts for some other bands which are not observed in the experimental spectra. It is reasonable to assume that this is due to the low intensities of these vibrations. Actually, the shifts were experimentally registered only for those bands whose calculated intensities are greater than 10 km mol^{-1}. The intensities of the 1353 cm^{-1} band of the quinone monomer and of the 1045 and 1042 cm^{-1} bands of the pyrimidine monomer (calculated wavenumbers) are much smaller (Table 7). This is probably why the corresponding dimer bands are not observed in the IR spectra. For the 804 cm^{-1} band of the pyrimidine monomer, the calculations predict shifts of +4.9 and −0.4 cm^{-1} in the PlanarB and Stacked dimers, respectively. However, this band is weak in the experimental spectrum (Table 1). We suspect that the band is shifted to higher frequencies due to dimer formation, but owing to its low intensity we could not definitely identify the shifted band. The calculations also predict shifts for three bands of the quinone monomer that are inactive in the IR spectra (3033, 1801, and 1375 cm^{-1}).

The potential energy distribution (PED) analysis (Tables 1S−4S) allows us to assign the observed bands of the PlanarB quinone−pyrimidine dimer. Two dimer bands at 886 and 719 cm^{-1} correspond to out-of-plane vibrations of the quinone and pyrimidine molecules in the dimer, respectively. The PED analysis of these vibrations indicates that the two vibrations have complicated forms: both the ring and C−H bond out-of-plane deformations contribute to the vibrations. The rest of the observed bands correspond to three in-plane vibrations of quinone and to four in-plane vibrations of pyrimidine.

Thus, the comparison between the observed and calculated frequency shifts of the two dimers allows us to suggest that the PlanarB dimer is primarily responsible for them.

7. Reaction Field Calculations

In this work we investigated the structure and relative stabilities of the weakly bonded quinone−pyrimidine dimers. The interaction energies between monomers were found to be within 20 kJ mol^{-1}. One can anticipate that these energies are comparable to the interaction energies between the dimers and the matrix itself. Thus, it would be interesting to evaluate the matrix influence on the relative stabilities of the dimers.

Accounting for matrix effects on the structure of molecules or their complexes is very complicated. Crystals of inert gases having dielectric constants from 1.24 (neon) to 2.22 (xenon)[17] may differently influence the relative energies of complexes with different structures and different dipole moments. On the other hand, local interactions with atoms of the matrix may change the structures of the complexes. Some theoretical calculations of intermolecular complexes including inert gas atom(s) were performed recently.[18,19] It was found that the calculations which in some way account for the interaction of the studied complex with the matrix correlate much better with results obtained from matrix isolation experiments.

We have made some attempt to account for the influence of the argon matrix on the relative stability of the PlanarB and Stacked quinone−pyrimidine dimers in the following way. Considering the matrix as a medium with a certain dielectric constant (ϵ), the interaction energies of the matrix and the dimers were calculated at the MP2/6-31++G** level of theory. The matrix effect was accounted for within Onsager's self-consistent reaction field model.[10] The dielectric constants of argon

TABLE 8: Quinone−Pyrimidine Dimer Energies from Reaction Field Calculations

	PlanarB	Stacked
a_0,[a] Å	4.72	4.70
dipole moment, D	2.64	3.13
total MP2(SCRF)/ 6-31++G** energy, au	−643.939 779 0	−643.942 517 8
MP2/6-31++G**energy, au	−643.939 083 5	−643.941 637 7
ΔE(MP2(SCRF)-MP2), kJ mol^{-1}	1.83	2.31
MP2(SCRF)+BSSE+ZPE, au	−643.779 086 5	−643.776 652 9
ΔE(MP2(SCRF)+BSSE+ZPE), kJ mol^{-1}	0.00	6.38

[a] The radii are 0.5 Å larger than the radii corresponding to the computed volumes, as is recommended.[16]

matrices have not been precisely determined; the ϵ value of the solid argon[17] being approximately 2 was used in the calculations. The dipole moment of the dimers investigated are listed in Table 3. The volumes occupied by the dimers were calculated at the SCF/6-31++G** level as the volumes inside a contour of 0.001 electron·bohr^{-3} density with the Monte Carlo integration procedure as implemented in the Gaussian92 program.[16] The values of occupied volumes were then used to estimate the cavity radii which are presented in Table 8. Finally, the MP2-(SCRF)/6-31++G** energies were calculated for the PlanarB and Stacked dimers. The results of the calculations are given in Table 8. The energy differences between the dimers in the matrix and in the gas phase are found to be rather small: −1.83 kJ mol^{-1} for the PlanarB dimer and −2.31 kJ mol^{-1} for the Stacked dimer, respectively. These values are nearly proportional to the dimer dipole moments. The decrease of the relative energy between the two dimers due to the matrix influence is only 0.49 kJ mol^{-1}; the PlanarB dimer is still the most stable quinone−pyrimidine configuration.

From these calculations we can conclude that Onsager's model predicts much smaller interaction energies between the dimer and the matrix than the quinone−pyrimidine interaction energies in the dimers. Thus, the relative stability of the different structures in an Ar matrix is essentially the same as in the gas phase.

8. Conclusions

We have applied matrix isolation IR spectroscopy and theoretical *ab initio* calculations to obtain information about the structure of weakly bonded quinone−pyrimidine complexes. A set of quinone−pyrimidine heterodimer bands was found in the fingerprint regions of the matrix IR spectra. The half-widths of the heterodimer bands were found to be similar to the half-widths of the bands of monomers, suggesting that the quinone−pyrimidine dimers have well-defined structures in the matrices. The observed shifts of the monomer bands due to the dimer formation do not exceed 10 cm^{-1}.

In a search for stable quinone−pyrimidine configurations, we used at first the SCF method with the 6-31++G** basis set. This method failed to predict a stable stacked configuration, although it produced reasonable interaction energies for the planar quinone−pyrimidine dimers. The geometries of two planar dimers and the stacked dimers were calculated at the MP2/6-31+G* level. We demonstrated that accounting for BSSE is important for predicting the relative stabilities of the planar and stacked dimers. The PlanarB complex was predicted to be the most stable, although the energy differences between all dimers are rather small.

The experimentally observed bands of the quinone−pyrimidine dimers were analyzed on the basis of harmonic frequency calculations performed for the PlanarB and Stacked dimers. Good agreement between frequency shifts observed in the IR spectra and theoretically predicted for the PlanarB dimer was found. It is therefore suggested that this dimer is responsible for most of the experimentally observed bands.

Acknowledgment. This work was supported in part by a COBASE grant allowing the visit of Dr. S. Stepanian to the University of Arizona. We also wish to express our gratitude to the International Science Foundation (Grant K35100) and to Ukranian State Committee of Science and Technology (Grant 2.3/809) for support of the work.

Supporting Information Available: Tables of the potential energy distribution analysis for the vibrations of pyrimidine and quinone monomers as well as those of the quinone−pyrimidine Stacked and *Planar A* dimers (6 pages). Ordering information is given on any current masthead page.

References and Notes

(1) Saenger, W. *Principles of Nucleic Acid Structure*; Springer-Verlag: New York, 1984.
(2) Murphy, C. J.; Arkin, M. R.; Jenkins, Y.; Ghatlia, N. D.; Bossmann, S. H.; Turro, N. J.; Barton J. K. *Science* **1993**, *262*, 1025.
(3) Dandliker, P. J.; Holmlin, R. E.; Barton, J. K. *Science* **1997**, *275*, 1465.
(4) (a) Sponer, J.; Leszczynski, J.; Hobza, P. *J. Comput. Chem.* **1996**, *17*, 841. (b) Hobza, P.; Sponer, P.; Polasek, M. *J. Am. Chem. Soc.* **1995**, *117*, 792. (c) Sponer, J.; Leszczynski, J.; Hobza, P. *J. Phys. Chem.* **1996**, *100*, 5590.
(5) Sponer, J.; Leszczynski, J.; Hobza, P. *J. Biomol. Struct. Dyn.* **1996**, *13*, 695.
(6) Sponer, J.; Hobza, P. *Chem. Phys. Lett.* **1997**, *267*, 263.
(7) McCarthy, W.; Smets, J.; Adamowicz, L.; Plokhotnichenko, A. M.; Radchenko, E. D.; Sheina, G. G.; Stepanian S. G. *Mol. Phys.*, **1**, in press.
(8) Gallois, B.; Langlois D'Estaintot, B.; Brown, T.; Hunter, W. N. *Acta Crystallogr.* **1993**, *D49*, 311.
(9) Leonard, G. A.; Hambley, T. W.; McAnlye-Hecht, K.; Brown, T.; Hunter, W. N. *Acta Crystallogr.* **1993**, *D49*, 458.
(10) Onsager, L. *J. Am. Chem. Soc.* **1936**, *58*, 1486.
(11) Radchenko, E. D.; Sheina, G. G.; Smorygo, N. A.; Blagoi, Yu. P. *J. Mol. Struct.* **1984**, *158*, 387.
(12) Reva, I. D.; Plokhotnichenko, A. M.; Radchenko, E. D.; Sheina, G. G.; Blagoi, Yu. P. *Spectrochim. Acta* **1994**, *50A*, 1107.
(13) Plokhotnichenko, A. M.; Ivanov, A. Yu.; Radchenko, E. D.; Sheina, G. G.; Blagoi, Yu. P. *Low Temp. Phys.* **1993**, *19*, 732.
(14) (a) Binkley, J. S.; Pople, J. A. *Int. J. Quantum Chem.* **1975**, *9*, 229. (b) Pople, J. A.; Binkley, J. S.; Seeger, R. *Int. J. Quantum Chem., Quantum. Chem. Symp.* **1976**, *10*, 1.
(15) Boys, S. F.; Bernardi, F. *Mol. Phys.* **1970**, *19*, 553.
(16) Frisch, M. J.; Trucks, G. W.; Head-Gordon, M.; Gill, P. M. W.; Wong, M. W.; Foresman, J. B.; Johnson, B. G.; Schlegel, H. B.; Robb, M. A.; Replogle, E. S.; Gomperts, R.; Andres, J. L.; Raghavachari, K.; Binkley, J. S.; Gonzalez, C.; Martin, R. L.; Fox, D. J.; Defrees, D. J.; Baker, J.; Stewart, J. J. P.; Pople, J. A. *Gaussian 92, Revision G.2*; Gaussian Inc.: Pittsburgh, PA, 1992.
(17) Verkin, B. I.; Prikhot'ko, A. F. *Cryocrystals* (in Russian); Naukova dumka: Kiev, Ukraine, 1983.
(18) Smets, J.; Destexhe, A.; Adamowicz, L.; Maes, G. *J. Phys. Chem. B* **1997**, *101*, 6583.
(19) Del Bene, J. E.; Szczepaniak, K.; Chabrier, P.; Person, W. B. *Chem. Phys. Lett.* **1997**, *264*, 109.